

STATISTICAL ANALYSIS OF THE LMS ALGORITHM APPLIED TO SUPER-RESOLUTION VIDEO RECONSTRUCTION

Guilherme H. Costa*

Department of Electrical Engineering
Federal University of Santa Catarina
Florianópolis, SC - Brazil

José C. M. Bermudez†

Department of Electrical Engineering
Federal University of Santa Catarina
Florianópolis, SC - Brazil

ABSTRACT

Super-resolution reconstruction of image sequences is highly dependent on the quality of the motion estimation between successive frames. This work presents a statistical analysis of the Least Mean Square (LMS) algorithm applied to super-resolution reconstruction of an image sequence. Deterministic recursions are derived for the mean and mean square behaviors of the reconstruction error as functions of the registration errors. The new model describes the behavior of the algorithm in realistic situations, and significantly improves the accuracy of a simple model available in the literature. Monte Carlo simulations show good agreement between actual and predicted behaviors.

1. INTRODUCTION

An approach to improve digital image quality which has attracted large interest in the last decade uses super-resolution reconstruction (SRR). SRR consists basically of combining multiple low-resolution images of the same scene or object to form a higher resolution image. Reference [1] reviews several important results on SRR available in the literature.

One of the major issues regarding SRR algorithms is their dependence on an accurate registration [2, 3, 4]. Wang and Qi [3] proposed a robust SRR algorithm based on Kalman filtering. The registration uncertainties are included in the filter equations, based on the estimation of the dynamical model errors due to the registration errors. Even though the results obtained in [3] are promising, convergence and computational complexity issues still need to be addressed. In [4], Lee and Kang define a constrained least-squares problem in which a signal dependent regularization functional, which incorporates the registration error, is inspired by regularized multi-channel image deconvolution techniques. A gradient descent algorithm is then employed to minimize the resulting cost function. The computational complexity is compatible with conventional SRR algorithms. In [5, 6], two adaptive algorithms based on the Kalman filtering have recently been proposed for SRR of image sequences. Differently from the traditional Kalman algorithm, no matrix inversion is required to reconstruct the high resolution image.

In spite of the justified concern about the robustness of SRR algorithms to registration errors, little has been done to theoretically quantify the effects of such errors on the reconstructed image or sequence. Most of the times, different solutions to the SRR problem

are compared based on subjective observations of the results or by emphasizing distinct areas of application [3, 4]. In [5, 7], a very simplified performance analysis of the adaptive SRR algorithms is presented. The analysis, however, is limited to convergence conditions and considers a worst case behavior under very restrictive circumstances. These results tell very little about the behavior of the algorithms in practical situations.

This work is a contribution to the quantification of the sensitivity of SRR methods to errors in the image registration process. The application of interest is the real-time SRR of image sequences, for which fast and accurate registration tends to be more important for performance than in the case of still images [2, 3, 4]. The least-mean-square algorithm proposed in [5, 6] (here called LMS-SRR) is analyzed and a deterministic model for its stochastic behavior is proposed. The new model permits the determination of the mean-square high-resolution estimation error for a given level of registration error.

In Section 2, we re-derive the LMS-SRR algorithm [5] by applying the stochastic gradient approach directly to the original image estimation problem. In Section 3, we present the statistical analysis and derive the analytical model for the algorithm behavior. In Section 4 we present simulation results to verify the accuracy of the theoretical model. In this paper, low-resolution (observed) images and high-resolution images will be referred to as LR and HR images, respectively.

2. THE LMS-SRR ALGORITHM

2.1. The signal models

Given the $N \times N$ matrix representation of an LR (observed) digital image $\mathbf{Y}(t)$ and an $M \times M$ ($M > N$) matrix representation of the original HR digital image $\mathbf{X}(t)$, the acquisition process can be expressed as

$$\mathbf{y}(t) = \mathbf{D}(t)\mathbf{x}(t) + \mathbf{e}(t), \quad (1)$$

where vectors $\mathbf{y}(t)$ ($N^2 \times 1$) and $\mathbf{x}(t)$ ($M^2 \times 1$) are the lexicographic representations of the degraded and original images, respectively, at time instant t . $\mathbf{D}(t)$ is an $N^2 \times M^2$ matrix that models the degradation due to sub-sampling and blurring, assumed to be known. The $N^2 \times 1$ vector $\mathbf{e}(t)$ models the observation (electronic) noise, which is assumed stationary in space, statistically independent of $\mathbf{y}(t)$ and $\mathbf{x}(t)$, white, Gaussian, with zero mean and with space autocorrelation matrix $\mathbf{R}_{\mathbf{e}}(t) = \sigma_e^2(t)\mathbf{I}$. $\sigma_e^2(t)$ is assumed to be determined from camera tests [8].

The dynamics of the input signal is modelled by

$$\mathbf{x}(t) = \mathbf{G}(t)\mathbf{x}(t-1) + \mathbf{s}(t), \quad (2)$$

*e-mail: holsbach@eel.ufsc.br. This work was supported by CNPq under grant 141456/2003-5.

†e-mail: j.bermudez@ieee.org. This work has been supported in part by CNPq under grants 308095/2003-0 and 472762/2003-6

Table 1. LMS algorithm applied to SRR

Initialization:

- Initialize K (Number of iterations for each t)
- $\hat{\mathbf{x}}_0(0) =$ interpolation of $\mathbf{y}(0)$

Algorithm:

$$\left\{ \begin{array}{l} \text{Loop in } t = 0, 1, 2, \dots \\ \left\{ \begin{array}{l} \text{Loop in } k = 0, 1, \dots, K-1 \\ \hat{\mathbf{x}}_{k+1}(t) = \hat{\mathbf{x}}_k(t) + \mu \mathbf{D}^T(t) [\mathbf{y}(t) - \mathbf{D}(t) \hat{\mathbf{x}}_k(t)] \\ \hat{\mathbf{x}}_0(t+1) = \mathbf{G}(t+1) \hat{\mathbf{x}}_K(t) \end{array} \right. \end{array} \right.$$

where $\mathbf{G}(t)$ is the warp matrix that describes the relative displacement from $\mathbf{x}(t-1)$ to $\mathbf{x}(t)$. In this paper we assume the occurrence of whole-image translational movement only. This is the simplest case to handle and can be assumed in several practical applications [9, 10]. Vector $\mathbf{s}(t)$ models the innovations in $\mathbf{x}(t)$.

The construction of the warp matrix $\mathbf{G}(t)$ depends on the technique used to handle the boundary conditions after image warping. For SRR, the best perceptual results are usually achieved assuming the Neumann conditions [11]. To simplify the mathematical modeling, we assume circular periodicity in the analysis. Simulation results will show that the effect of this simplifying assumption is not significant in determining the actual algorithm behavior.

2.2. The LMS-SRR adaptive algorithm

Several SRR solutions are based on the minimization of the norm $\|\epsilon(t)\| = \|\mathbf{y}(t) - \mathbf{D}(t)\hat{\mathbf{x}}(t)\|$ [1, and references therein], where $\hat{\mathbf{x}}(t)$ is the estimated image and $\epsilon(t)$ is the estimate of the observation noise vector. The LMS-SRR algorithm attempts to minimize the mean-square error (MSE) $E\{\|\epsilon(t)\|^2\}$ [6], where $E\{\cdot\}$ denotes statistical expectation. Thus, the cost function is defined as $\mathbf{J}_{\text{MS}}(t) = E\{\|\epsilon(t)\|^2 | \hat{\mathbf{x}}(t)\}$. According to the steepest descent method, the updating of the estimate $\hat{\mathbf{x}}(t)$ to minimize $\mathbf{J}_{\text{MS}}(t)$ is in the negative direction of its gradient. Thus,

$$\nabla \mathbf{J}_{\text{MS}}(t) = \frac{\partial \mathbf{J}_{\text{MS}}(t)}{\partial \hat{\mathbf{x}}(t)} = -2\mathbf{D}^T(t) \{E[\mathbf{y}(t)] - \mathbf{D}(t)\hat{\mathbf{x}}(t)\} \quad (3)$$

and the recursive update equation for $\hat{\mathbf{x}}(t)$ is given by $\hat{\mathbf{x}}_{k+1}(t) = \hat{\mathbf{x}}_k(t) - (\mu/2)\nabla \mathbf{J}_{\text{MS}}(t)$. Notice that the performance surface $\mathbf{J}_{\text{MS}}(t)$ is defined for a specific time instant t .

Approximating the steepest descent algorithm by its stochastic version leads to the LMS-SRR adaptive algorithm. Approximating (3) by its instantaneous estimate [12] yields

$$\hat{\mathbf{x}}_{k+1}(t) = \hat{\mathbf{x}}_k(t) + \mu \mathbf{D}^T(t) [\mathbf{y}(t) - \mathbf{D}(t)\hat{\mathbf{x}}_k(t)], \quad (4)$$

which is the stochastic recursion for the LMS-SRR adaptive algorithm. The time update of (4) is based on the signal dynamics (2), which is determined by the warp matrix $\mathbf{G}(t)$. The complete LMS-SRR algorithm is described in Table 1.

3. STATISTICAL ANALYSIS

Hereafter $\mathbf{G}(t)$ will be considered deterministic and will represent the warp matrix free from displacement estimation errors. The matrix $\hat{\mathbf{G}}(t)$ will represent the estimated warp matrix. Considering that

only the estimate $\hat{\mathbf{G}}(t)$ is available during the reconstruction process, the time update equation of the actual LMS-SRR algorithm is given by:

$$\hat{\mathbf{x}}_0(t+1) = \hat{\mathbf{G}}(t+1)\hat{\mathbf{x}}_K(t), \quad (5)$$

where $\hat{\mathbf{G}}(t)$ can be modelled as [5, 4]

$$\hat{\mathbf{G}}(t) = \mathbf{G}(t) + \Delta \mathbf{G}(t). \quad (6)$$

where $\Delta \mathbf{G}(t)$ is a random matrix with properties determined by the registration method and by the image sequence. Grouping together (4) and (5) leads to the recursive equation that describes the LMS-SRR- K algorithm, with K iterations by time sample:

$$\hat{\mathbf{x}}(t) = \mathbf{A}^K \hat{\mathbf{G}}(t) \hat{\mathbf{x}}(t-1) + \mu \sum_{n=0}^{K-1} \mathbf{A}^n \mathbf{D}^T(t) \mathbf{y}(t), \quad (7)$$

where $\mathbf{A} = [\mathbf{I} - \mu \mathbf{D}^T(t) \mathbf{D}(t)]$.

Let us define the HR image estimation error as $\mathbf{v}(t) = \hat{\mathbf{x}}(t) - \mathbf{x}(t)$. From (1), (2), (6) and (7) it can be shown that

$$\begin{aligned} \mathbf{v}(t) &= \mathbf{A}^K \mathbf{G}(t) \mathbf{v}(t-1) + \mathbf{A}^K \Delta \mathbf{G}(t) \hat{\mathbf{x}}(t-1) \\ &\quad - \mathbf{A}^K \mathbf{s}(t) + \mu \sum_{n=0}^{K-1} \mathbf{A}^n \mathbf{D}^T(t) \mathbf{e}(t). \end{aligned} \quad (8)$$

Eq. (8) can be used to determine the mean and fluctuation behaviors of the HR image reconstruction error $\mathbf{v}(t)$.

3.1. Statistical assumptions and approximations

The following approximations and assumptions are used in the following statistical analysis: (A1) The vector $\Delta \mathbf{G}(t) \hat{\mathbf{x}}(t-1)$ is assumed to be zero-mean, i.i.d. with $M^2 \times M^2$ autocorrelation matrix $\mathbf{R}_r(t) = \sigma_r^2(t) \mathbf{I}$ and statistically independent of the observation noise vector $\mathbf{e}(t)$. This assumption has been used in [3] with good results; (A2) The effect of outliers in the dynamics of the image are neglected. It tends to lead to better results as the size of the image increases. Thus, (2) is approximated by $\mathbf{x}(t) \simeq \mathbf{G}(t)\mathbf{x}(t-1)$; (A3) The effects of the statistical dependence between the registration error matrix $\Delta \mathbf{G}(t)$ and the HR images $\mathbf{x}(t-1)$ and $\hat{\mathbf{x}}(t-1)$ are neglected. The impact of this assumption on the validity of the analytical model will depend on the specific registration algorithm used; (A4) The observation noise vector $\mathbf{e}(t)$ is assumed to be statistically independent of the registration errors $\Delta \mathbf{G}(t)$ and of any other signal in the system.

3.2. The mean reconstruction error behavior

Taking the expected value of (8) and using A1–A4 yields a model for the mean behavior of the HR image reconstruction error:

$$E[\mathbf{v}(t)] = [\mathbf{I} - \mu \mathbf{D}^T(t) \mathbf{D}(t)]^K \mathbf{G}(t) E[\mathbf{v}(t-1)]. \quad (9)$$

3.3. The mean-square reconstruction error behavior

The fluctuations of the reconstruction error about the mean can be studied through the squared norm of $\mathbf{v}(t)$, $E[\mathbf{v}^T(t)\mathbf{v}(t)]$. This norm can be evaluated as $\text{tr}\{E[\mathbf{v}(t)\mathbf{v}^T(t)]\} = \text{tr}\{\mathbf{K}(t)\}$, where $\mathbf{K}(t)$ is the autocorrelation matrix of $\mathbf{v}(t)$ and $\text{tr}\{\cdot\}$ denotes the trace of a matrix.

Post-multiplying (8) by its transpose, taking the expected value, and using A1–A4 and (6) yields

$$\begin{aligned} \mathbf{K}(t) &= \mathbf{A}^K \{ \mathbf{G}(t) \mathbf{K}(t-1) \mathbf{G}^T(t) + \mathbf{R}_r(t) \\ &+ \mathbf{G}(t) \mathbb{E}[\mathbf{v}(t-1) \hat{\mathbf{x}}^T(t-1)] \{ \mathbb{E}[\hat{\mathbf{G}}^T(t)] - \mathbf{G}^T(t) \} \\ &+ \{ \mathbb{E}[\hat{\mathbf{G}}(t)] - \mathbf{G}(t) \} \mathbb{E}[\hat{\mathbf{x}}(t-1) \mathbf{v}^T(t-1)] \mathbf{G}^T(t) \} \mathbf{A}^K \\ &+ \mu^2 \sum_{n=0}^{K-1} \mathbf{A}^n \mathbf{D}^T(t) \mathbf{R}_e(t) \mathbf{D}(t) \sum_{n=0}^{K-1} \mathbf{A}^n. \end{aligned} \quad (10)$$

The evaluation of the second and third lines of (10) requires de evaluation of $\mathbb{E}[\hat{\mathbf{x}}(t) \mathbf{v}^T(t)]$. Since $\mathbf{v}(t) = \hat{\mathbf{x}}(t) - \mathbf{x}(t)$, this expectation can be written as

$$\mathbb{E}[\hat{\mathbf{x}}(t) \mathbf{v}^T(t)] = \mathbf{K}(t) + \mathbf{R}_{\mathbf{x}\hat{\mathbf{x}}}(t) - \mathbf{R}_x(t), \quad (11)$$

where $\mathbf{R}_{\mathbf{x}\hat{\mathbf{x}}}(t) = \mathbb{E}[\mathbf{x}(t) \hat{\mathbf{x}}^T(t)]$ and $\mathbf{R}_x(t) = \mathbb{E}[\mathbf{x}(t) \mathbf{x}^T(t)]$.

The matrix $\mathbf{R}_x(t)$ is a function of the HR image to be estimated. The cross-correlation matrix $\mathbf{R}_{\mathbf{x}\hat{\mathbf{x}}}(t)$ can be determined recursively. Using (7), (1), A2–A4 and the zero-mean property of $\mathbf{e}(t)$,

$$\begin{aligned} \mathbf{R}_{\mathbf{x}\hat{\mathbf{x}}}(t) &= \mathbf{G}(t) \mathbf{R}_{\mathbf{x}\hat{\mathbf{x}}}(t-1) \mathbb{E}[\hat{\mathbf{G}}^T(t)] \mathbf{A}^K \\ &+ \mu \mathbf{R}_x(t) \mathbf{D}^T(t) \mathbf{D}(t) \sum_{n=0}^{K-1} \mathbf{A}^n. \end{aligned} \quad (12)$$

An expression for the correlation matrix $\mathbf{R}_r(t)$ is also needed in (10). Considering A1, $\sigma_r^2(t) = \text{tr}[\mathbf{R}_r(t)]/M^2$, where M^2 is the number of pixels of the high resolution images. Using A3 and the commutative property of the trace of a product of matrices, we have

$$\text{tr}[\mathbf{R}_r(t)] = \text{tr}\{ \mathbf{R}_{\hat{\mathbf{x}}}(t-1) \mathbb{E}[\Delta \mathbf{G}^T(t) \Delta \mathbf{G}(t)] \}, \quad (13)$$

where $\mathbf{R}_{\hat{\mathbf{x}}}(t) = \mathbb{E}[\hat{\mathbf{x}}(t) \hat{\mathbf{x}}^T(t)]$. Manipulating algebraically the expression of $\mathbf{R}_{\hat{\mathbf{x}}}(t)$, as in (11), yields $\mathbf{R}_{\hat{\mathbf{x}}}(t) = \mathbf{K}(t) + \mathbf{R}_{\mathbf{x}\hat{\mathbf{x}}}(t) + \mathbf{R}_{\mathbf{x}\hat{\mathbf{x}}}(t) - \mathbf{R}_x(t)$.

Form (6), the expected value $\mathbb{E}[\Delta \mathbf{G}^T(t) \Delta \mathbf{G}(t)]$ in (13) can be written as

$$\begin{aligned} \mathbb{E}[\Delta \mathbf{G}^T(t) \Delta \mathbf{G}(t)] &= \mathbb{E}[\hat{\mathbf{G}}^T(t) \hat{\mathbf{G}}(t)] - \mathbb{E}[\hat{\mathbf{G}}^T(t)] \mathbf{G}(t) \\ &- \mathbf{G}^T(t) \mathbb{E}[\hat{\mathbf{G}}(t)] + \mathbf{G}^T(t) \mathbf{G}(t). \end{aligned} \quad (14)$$

Finally, the expected values $\mathbb{E}[\hat{\mathbf{G}}(t)]$ and $\mathbb{E}[\hat{\mathbf{G}}^T(t) \hat{\mathbf{G}}(t)]$, which appear in (10)–(14), must be estimated based on the characteristics of the registration algorithm used and on the statistical properties of the image sequence. Next section discusses the estimation of these moments for some particular cases of practical interest.

3.4. Implementation

We show in this section that $\mathbb{E}[\hat{\mathbf{G}}(t)]$ and $\mathbb{E}[\hat{\mathbf{G}}^T(t) \hat{\mathbf{G}}(t)]$ can be estimated with reasonable computational cost when: (i) The relative motion between the images is global and translational with integer steps in the HR grid; (ii) $\mathbf{G}(t)$ is built assuming circular periodicity of the image to determine the boundary pixels after movement.

Under these conditions, $\mathbf{G}(t)$ works like a permutation matrix to the rows of $\mathbf{x}(t)$, in (2), and therefore is full rank. Thus, the estimated warp matrix $\hat{\mathbf{G}}(t)$ can be also represented as a matrix product:

$$\hat{\mathbf{G}}(t) = \mathbf{G}(t) + \Delta \mathbf{G}(t) = \tilde{\mathbf{G}}(t) \mathbf{G}(t). \quad (15)$$

In order to solve (14), follows from (15) that $\mathbb{E}[\hat{\mathbf{G}}(t)] = \mathbb{E}[\tilde{\mathbf{G}}(t)] \mathbf{G}(t)$ and $\mathbb{E}[\hat{\mathbf{G}}^T(t) \hat{\mathbf{G}}(t)] = \mathbf{G}^T(t) \mathbb{E}[\tilde{\mathbf{G}}^T(t) \tilde{\mathbf{G}}(t)] \mathbf{G}(t)$. Assuming that

Table 2. LMS algorithm applied to SRR

| | |
|--|--|
| <p>Initialization:</p> <p>$\mathbf{R}_{\mathbf{x}\hat{\mathbf{x}}}(0) = \mathbf{0}$; $\hat{\mathbf{x}}(1) = \text{interpolation of } \mathbf{y}(1)$ $\mathbf{v}(1) = \hat{\mathbf{x}}(1) - \mathbf{x}(1)$; $\mathbf{K}(1) = \mathbf{v}(1) \mathbf{v}^T(1)$ $L = \text{number of iterations to Monte Carlo simulations}$ $\mathbb{E}[\hat{\mathbf{G}}(t)] \simeq \frac{1}{L} \sum_{i=1}^L \tilde{\mathbf{G}}(i)$ $\mathbb{E}[\hat{\mathbf{G}}^T(t) \hat{\mathbf{G}}(t)] \simeq \frac{1}{L} \sum_{i=1}^L \tilde{\mathbf{G}}^T(i) \tilde{\mathbf{G}}(i)$ $\mathbb{E}[\hat{\mathbf{G}}(1)] = \mathbb{E}[\tilde{\mathbf{G}}(1)] \mathbf{G}(1)$</p> <p>Algorithm:</p> <p>Loop in $t = 2, 3, 4, \dots$</p> <p style="margin-left: 20px;">Compute $\mathbf{R}_{\mathbf{x}\hat{\mathbf{x}}}(t-1)$ via Eq. (12) Compute $\mathbb{E}[\Delta \mathbf{G}^T(t) \Delta \mathbf{G}(t)]$ via Eq. (14) Compute $\sigma_r^2(t) = \text{tr}[\mathbf{R}_r(t)]/M^2$ via Eq. (13) Compute $\mathbf{R}_r(t) = \sigma_r^2(t) \mathbf{I}$ Compute $\mathbb{E}[\hat{\mathbf{x}}(t-1) \mathbf{v}^T(t-1)]$ via Eq. (11) Compute $\mathbf{K}(t)$ via Eq. (10)</p> | |
|--|--|

the image sequence we want to reconstruct is stationary (for example, when the camera motion is around an object), it is reasonable to expect the motion estimation error to be also stationary. Then, $\mathbb{E}[\hat{\mathbf{G}}(t)]$ and $\mathbb{E}[\hat{\mathbf{G}}^T(t) \hat{\mathbf{G}}(t)]$ are not functions of t and can be estimated *a priori* and used in all iterations of the recursive model, reducing considerably the computational cost. The final algorithm to determine $\mathbf{K}(t)$ is detailed in Table 2.

4. SIMULATION RESULTS

In all simulations presented in this section, we have used $M = 20$, $N = 10$, $L = 500$ and $\sigma_e^2(t) = 10$. The global displacement vectors $\mathbf{d}(t) = [d_r(t), d_c(t)]$ were generated from a random walk process. Such vectors were considered known *a priori*. The registration error $\Delta \mathbf{d}(t) = [\Delta d_r(t), \Delta d_c(t)]$ was assumed zero-mean Gaussian noise. This assumption yields good results even for registration algorithms for which this error is known to be non-Gaussian [13]. $\Delta d_r(t)$ and $\Delta d_c(t)$ are assumed independent of each other, with variances $\sigma_{\Delta d_r}^2$ and $\sigma_{\Delta d_c}^2$ estimated from the registration algorithm. Blurring is not considered, but could be easily incorporated into $\mathbf{D}(t)$. $\mathbf{R}_x(t)$ has been estimated from the original HR images at each time instant.

The registration algorithms proposed in [14] and [13] were considered in the simulations. The results were compared with the known motion case (free from estimation errors). For the algorithm in [14], the global velocity vector was estimated by the average pixel velocity vector.

The simulation results for the models in (9) and in Table 2 are presented in Figs. 1 and 2. The ensemble used to generate these figures was composed by several different scenes. Note that Fig. 1 presents only the central pixel error. Fig. 2 presents the fluctuations of the reconstruction error about the mean, divided by the number of pixels of the image. In the known motion case, the pixels from the five boundary rows and columns of the reconstructed (HR) image are not considered. This minimizes the discrepancies between simulation and theory caused by boundary effects. In the other cases, this effect can be neglected when compared to the registration error noise. The additive noise for the acquisition model (1) has been generated to obtain the following signal-to-noise rates: PSNR \simeq 38dB e SNR \simeq 23dB. These rates were computed considering the vectors $\mathbf{y}(t)$ and $\mathbf{D}(t) \mathbf{x}(t)$.

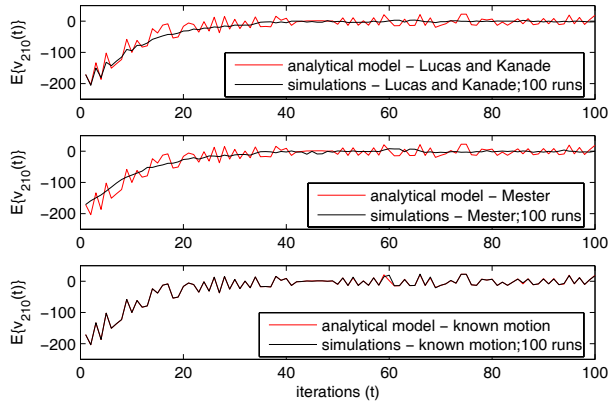


Fig. 1. Central pixel (210th element of $\mathbf{v}(t)$) mean reconstruction error: $K = 4$; $\mu = 0.1$.

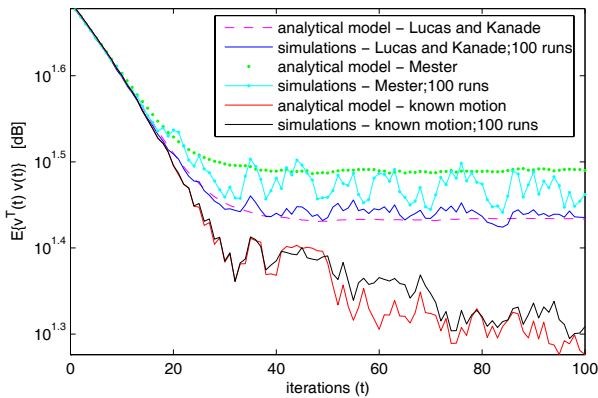


Fig. 2. Mean square reconstruction error: $K = 4$; $\mu = 0.1$.

For $\mathbf{D}(t) = \mathbf{I}$ we have the situation modelled in [5]. In this case, the results obtained using the model proposed here and the one from [5]) are compared in Fig. 3. Note that the new model provides a much superior estimation of the algorithm behavior.

5. CONCLUSIONS

This paper has presented an analytical model for predicting the stochastic behavior of the LMS algorithm proposed in [6]. Deterministic recursive equations were derived for the mean and mean-square reconstruction error as functions of the registration errors. The proposed model yields a very good agreement with Monte Carlo simulations in both transient and steady-state phases of adaption. Relative to the existing model [5], the new model: (i) estimates the algorithm behavior considering super-resolution (sub-sampling); (ii) estimates the mean and the fluctuation behaviors of the reconstruction error during transient and in steady-state.

6. REFERENCES

[1] S.C.Park, M.K. Park, and M.G. Kang, "Super-resolution image reconstruction: A technical overview," *IEEE Signal Processing Magazine*, vol. 20, no. 3, pp. 21–36, May 2003.

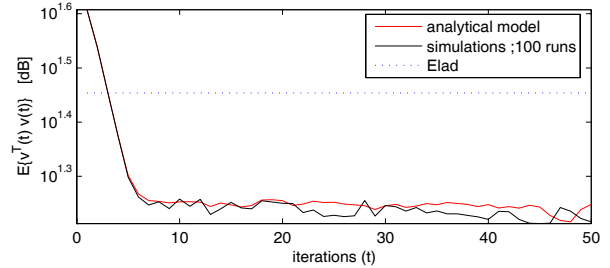


Fig. 3. Mean square reconstruction error: $\mathbf{D}(t) = \mathbf{I}$; $K = 1$; $\mu = 0.5$.

[2] D. Capel and A. Zisserman, "Computer vision applied to super resolution," *IEEE Signal Processing Magazine*, vol. 20, no. 3, pp. 75–86, May 2003.

[3] Z. Wang and F. Qi, "Super-resolution video restoration with model uncertainties," *IEEE Int'l Conf. Image Processing*, vol. 2, pp. 853–856, Sept. 2002.

[4] E.S. Lee and M.G. Kang, "Regularized adaptive high-resolution image reconstruction considering inaccurate sub-pixel registration," *IEEE Trans. Image Processing*, vol. 12, no. 7, pp. 826–837, July 2003.

[5] M. Elad, *Super-Resolution Reconstruction of images*, Ph.D. thesis, Israel Institute of Technology, Dec. 1996.

[6] M. Elad and A. Feuer, "Superresolution restoration of an image sequence: Adaptive filtering approach," *IEEE Trans. Image Processing*, vol. 8, no. 3, pp. 387–395, Mar. 1999.

[7] M. Elad and A. Feuer, "Superresolution reconstruction of an image sequence," *IEEE Trans. Pattern Analysis and Machine Intelligence*, vol. 21, no. 9, pp. 817–834, Sept. 1999.

[8] T. Ono, H. Hasegawa, I. Yamanda, and K. Sakaniwa, "An adaptive super-resolution of videos with noise information on camera systems," *IEEE Intl. Conf. Acoustics, Speech, and Signal Processing*, vol. 2, pp. 857–860, Mar. 2005.

[9] M. Elad and Y. Hel-Or, "A fast super-resolution reconstruction algorithm for pure translational motion and common space-invariant blur," *IEEE Trans. Image Processing*, vol. 10, no. 8, pp. 1187–1193, Aug. 2001.

[10] S.P. Kim, N.K. Bose, and H.M. Valenzuela, "Recursive reconstruction of high resolution image from noisy undersampled multiframe," *IEEE Trans. Acoustics, Speech, and Signal Processing*, vol. 38, no. 6, pp. 1013–1027, June 1990.

[11] M.K. Ng and N.K. Bose, "Analysis of displacement errors in high-resolution image reconstruction with multisensors," *IEEE Trans. Circuits and Systems*, vol. 49, no. 6, pp. 806–813, June 2002.

[12] Simon Haykin, *Adaptive Filter Theory*, Prentice Hall, New Jersey, 4th ed. edition, 2002.

[13] R. Mester and M. Hotter, "Robust displacement vector estimation including a statistical error analysis," *IEE Int'l Conf. Image Processing and its Applications*, pp. 168–172, July 1995.

[14] B.D. Lucas and T. Kanade, "An iterative image registration technique with an application to stereo vision," *DARPA Image Understanding Workshop*, pp. 121–130, Apr. 1981.